

Coherent pion photoproduction

V. Girija and V. Devanathan

Department of Nuclear Physics, University of Madras, Madras 600 025, India

A. Nagl and H. Überall

Department of Physics, The Catholic University of America, Washington D.C. 20064

(Received 8 March 1982)

The photoproduction of neutral pions is studied in the distorted wave impulse approximation. The cross sections are calculated for pion production from ${}^4\text{He}$, ${}^{12}\text{C}$, ${}^{16}\text{O}$, and ${}^{40}\text{Ca}$ and are found to be in good agreement with the available data. The present results compare well with the theoretical calculations carried out in the framework of the isobar-doorway model.

[NUCLEAR REACTIONS π^0 photoproduction from ${}^4\text{He}$, ${}^{12}\text{C}$, ${}^{16}\text{O}$,
 ${}^{40}\text{Ca}$; distorted wave impulse approximation.]

I. INTRODUCTION

Saunders¹ was the first to study the effect of the final state interaction of the pion with the residual nucleus. He observed that his distorted wave impulse approximation (DWIA) calculations for the coherent pion production from ${}^{12}\text{C}$, ${}^{40}\text{Ca}$, and ${}^{208}\text{Pb}$ yielded results which were much lower than the experimental data² available then. Subsequently, the phenomenological isobar-doorway model (IDM), which treats the isobars as nuclear constituents, was employed for a study of the reaction in ${}^{12}\text{C}$ using the isobar-nuclear form factor obtained by fitting the pion-nucleus elastic scattering data.³ The angular distribution for photon energy of 250 MeV showed a dip around 50° corresponding to the first diffractive minimum of the pion-nucleus elastic scattering cross sections. This is unavoidable when the total amplitude is parametrized by a single form factor. However, the IDM gave substantial cross sections for large angles, as shown by experiment. The model has recently been refined by Saharia and Woloshyn⁴ by modifying the transition operator to account for the many body effects. For this, they adopt the same method that is employed for the pion-nucleus optical potential.⁵ They also take into account the nonlocality associated with the isobar propagation and recoil corrections. With these modifications, they succeed in obtaining a fairly good fit to the existing data for neutral pion production from ${}^{12}\text{C}$ (Ref. 2) and ${}^4\text{He}$.⁶ It is also reported that the cross sections are not sensitive to the choice of a channel dependent or channel indepen-

dent parametrization. But the models are constrained to fit the pion-nucleus elastic scattering data. A comparison has also been made with the DWIA calculation carried out with the wave functions obtained by using the PIPIT code,⁷ and appreciable differences are found.

With the advent of high energy accelerators, the experimental situation is steadily improving and the results for the neutral pion production from ${}^{12}\text{C}$ for photon energy around 250 MeV were reported at the recent meeting in Versailles.^{8,9} The purpose of the present paper is to discuss the results of the present DWIA calculations performed with certain refinements and compare them with the existing data (Refs. 2, 6, 8, and 9). The coherent photopion production, which involves only the spin-independent term of the production amplitude and is free from the ambiguities of the nuclear structure, can shed light on the sensitivity of the cross sections to the pion-nucleus optical potentials.

II. THE FORMALISM

The transition amplitude for the process of coherent pion production from nuclei can be written as

$$T = \sum_j t_j = \sum_j \phi^*(\vec{\mu}, \vec{r}_j) t_s(j) \exp(i \vec{v} \cdot \vec{r}_j), \quad (1)$$

where the index j runs over the A nucleons. The final state interaction of the pion with the residual nucleus is contained in the distorted pion wave

function $\phi(\vec{\mu}, \vec{r}_j)$. The incident photon is represented by a plane wave. The quantity $t_s(j)$ denotes the single nucleon amplitude of which only the spin-independent part contributes for the spin zero nuclei

$$t_s = cc_5(\vec{\mu} \cdot \vec{v} \times \vec{\epsilon}) . \quad (2)$$

Using the production amplitudes of Berends *et al.*¹⁰ (BDW) and Chew *et al.*¹¹ (CGLN), we have, respectively,

$$c = \frac{2\pi}{(\mu_0 v_0)^{1/2}} \text{ and } c_5 = F_2 , \quad (3)$$

$$c = \frac{2\pi e f}{(\mu_0 v_0)^{1/2}} \text{ and } c_5 = \lambda h^{++} .$$

$\vec{\mu}$, μ_0 and \vec{v} , v_0 represent the momentum and ener-

gy of the pion and the photon, respectively. All other quantities are defined in Refs. 10 and 11. These production amplitudes are Lorentz-transformed to the laboratory system in the usual way. Expanding the pion wave functions into partial waves, we get

$$\phi(\vec{\mu}, \vec{r}_j) = 4\pi \sum_{l_\mu} (i)^{l_\mu} g_{l_\mu}(\mu r) \sum_{m_\mu} Y_{l_\mu}^{m_\mu}(\hat{r}) Y_{l_\mu}^{m_\mu*}(\hat{\mu}) . \quad (4)$$

The radial part of the pion wave function $g_{l_\mu}(\mu r)$ is obtained by solving the Klein-Gordon equation with a suitable pion-nucleus optical potential. Using the Rayleigh expansion for the photon wave functions and replacing the pion momentum by the gradient operator $\vec{\nabla}_\pi$, we have

$$t_j = 4\pi 2^{1/2} cc_5 \sum_{l_\mu, l_\nu} (i)^{l_\nu - l_\mu} (-1)^{l_\nu} \sum_L [\{ (\nu \times \epsilon)_1 \times Y_{l_\mu}(\hat{\mu}) \}_L \times Y_{l_\nu}(\hat{\nu})]_0^0 \delta_{L, l_\nu} R_1(l_\mu, L, r_j) , \quad (5)$$

where

$$R_1(l_\mu, L, r_j) = \{ (L)^{1/2} (D_- (l_\mu) g_{l_\mu}(\mu r_j))^* \delta_{L, l_\mu} + 1 - (L+1)^{1/2} (D_+ (l_\mu) g_{l_\mu}(\mu r_j))^* \delta_{L, l_\mu - 1} \} j_{l_\nu}(v r_j) . \quad (6)$$

We follow the notations and conventions of Rose¹² for angular momentum algebra. It is now easy to evaluate the transition operator between the ground states of the nucleus with the density distribution $\rho(r)$ (normalized to A) to obtain the matrix element Q :

$$Q = (4\pi)^2 (2)^{1/2} cc_5 \sum_{l_\mu, l_\nu, L} (i)^{l_\nu - l_\mu} (-1)^{l_\nu} S \delta_{L, l_\nu} \int \rho(r) R_1(l_\mu, L, r_j) r^2 dr , \quad (7)$$

where S is obtained by choosing the direction of the incident photon to be the z axis,

$$S = \frac{(-1)^{l_\nu}}{(4\pi)^{1/2}} \sum_m C(1l_\mu L, m - m 0) C(111, 0mm) v \epsilon_1^m Y_{l_\mu}^{-m}(\hat{\mu}) . \quad (8)$$

It is to be stressed that the transition operator can be evaluated numerically for a particular magnetic quantum number m and then squared bearing in mind the fact that

$$\epsilon_1^m \epsilon_1^{m'*} = \delta_{m, m'} \quad (\text{since } \epsilon_1^0 = 0) . \quad (9)$$

In the limiting case of plane waves for pions (PWIA), we get

$$t_j = t_s j_0(kr_j) , \quad (10)$$

where $\vec{k} = \vec{v} - \vec{\mu}$ and the matrix element now reduces to

$$Q = 4\pi t_s \int j_0(kr_j) \rho(r) r^2 dr . \quad (11)$$

The density distribution is a perfect Gaussian for ${}^4\text{He}$ and we assume the Fermi distribution for ${}^{12}\text{C}$, ${}^{16}\text{O}$, and ${}^{40}\text{Ca}$, with the parameters taken from elec-

tron scattering data. The oscillator wave functions are also used just to facilitate a comparative study.

The local and nonlocal parts of the pion-nucleus interaction are taken from the work of Stricker *et al.*,¹³ which accounts for the multiple scattering effects, takes care of the angle transformation, and takes into account the effects due to $\pi NN \rightarrow \pi NN$ processes and true pion absorption. This form of the potential has been very successful in reproducing the elastic scattering data at low energies and has been extrapolated for medium energies also. We utilize the parameters listed by Stricker *et al.*, making interpolations as and when necessary. The optical potential plays a crucial role in photopion reactions, since it takes care of the corrections due to the interaction of the propagating particle with other nucleons in nuclear medium, Pauli blocking, and binding energy effects, which are essential for

an off-shell extrapolation but are ignored in the impulse approximation theory. In coherent pion production, this optical potential is more or less the deciding factor for the cross sections, since the other two ingredients, viz., (a) nuclear structure and (b) the elementary spin-independent part of the amplitude, are quite easy to handle. If the transition operator is to be modified to account for these off-shell corrections, one has to carefully avoid double counting. Alternatively, the pion-nucleus optical potential constrained to fit the elastic scattering data is found to be successful in explaining the coherent pion cross sections.

III. RESULTS AND CONCLUSION

The results of our calculations obtained with the ingredients discussed above are presented in Figs. 1–9. The angular distributions for photon energies of 230 and 250 MeV for π^0 production from ^{12}C depicted in Figs. 1 and 2 show quite a good agreement with the data of Refs. 8 and 2. The measurements for gamma ray energy of 250 MeV reported in Ref. 9 are compatible with the old experimental data of Ref. 2 (as quoted by Saunders¹). The differential cross sections reported here are also consistent with the recent calculations of Saharia and Woloshyn.⁴ Figure 3 shows our present results for total cross sections for ^{12}C compared with the re-

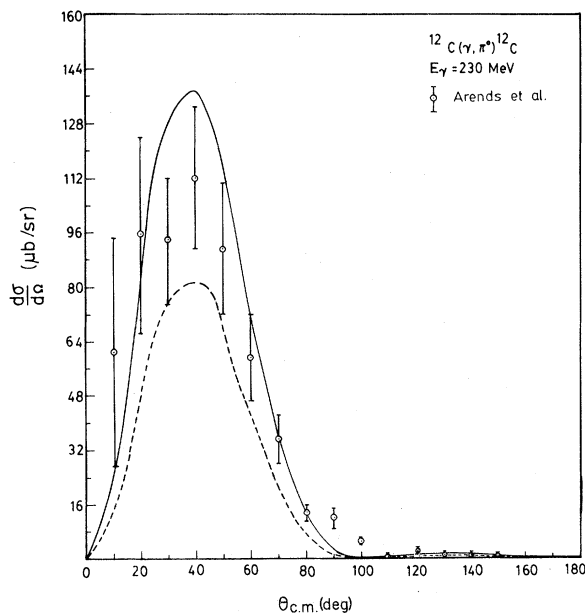


FIG. 1. Angular distribution for coherent pion production from ^{12}C for laboratory photon energy $E_\gamma = 230$ MeV. The data are from Ref. 8 for $E_\gamma = 235$ MeV. The continuous and dashed lines are obtained in DWIA with the CGLN and BDW amplitudes, respectively.

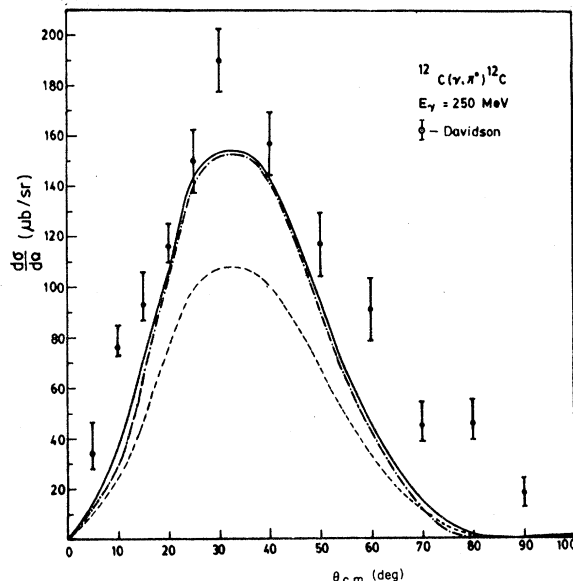


FIG. 2. Differential cross sections obtained in DWIA for $E_\gamma = 250$ MeV along with the data of Davidson as quoted by Saunders (Ref. 1). The solid line indicates CGLN, the dashed line indicates BDW. The IDM calculation of Saharia and Woloshyn is denoted by the dashed-dotted curve.

cent measurements of the Bonn group, in which the incoherent production has been subtracted out. It may be noted that the preliminary results for the differential and total cross sections reported in Ref. 8 are not consistent among themselves. That is the reason why the angular data of Ref. 8 integrate to fall below the BDW curve at 230 MeV in Fig. 3. The results for the reaction in ^{16}O are presented in Figs. 4 and 5. The pronounced differences in the cross sections obtained in DWIA (with PIPIT wave functions) and IDM, as reported by Saharia and Woloshyn, disappear in the present calculations. The difference mentioned above in the work of Saharia and Woloshyn may be because of the use of the PIPIT wave functions obtained by using the first order potential that does not reproduce the elastic scattering data well. The multipoles used in their work may also produce a difference.

The figures also reveal that the CGLN amplitude provides cross sections which are larger almost by a factor of 2 when compared to those obtained with the BDW amplitude for energies below resonance. This ratio decreases as one goes to the (3,3) resonance region, and for energies beyond the resonance, the cross sections obtained with the CGLN amplitude, are slightly lower. The same trend is observed in the cross sections obtained with the

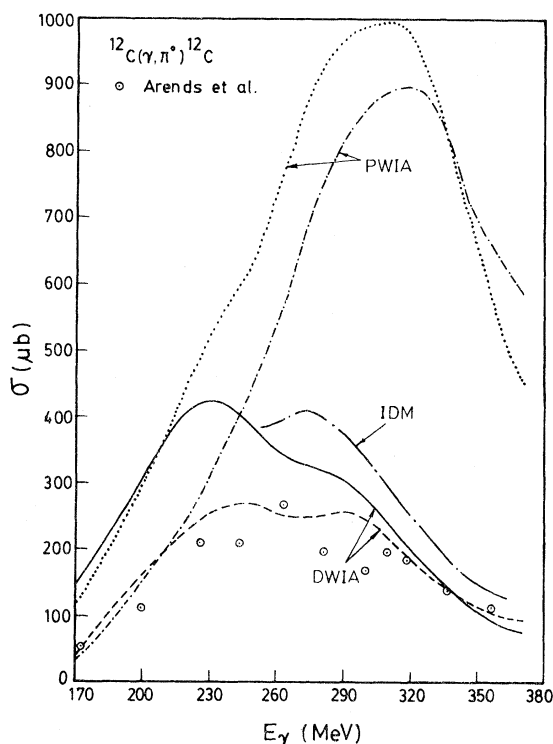


FIG. 3. Total cross sections for $^{12}\text{C}(\gamma, \pi^0)^{12}\text{C}$ compared with the recent data of Ref. 8. The dotted and continuous lines are used for the CGLN amplitude and the dashed-dotted and dashed lines indicate BDW amplitude. The IDM calculation of Saharia and Woloshyn is also shown.

CGLN and BDW amplitudes for π^0 production from single nucleons, although the difference is much smaller.¹⁴ The large discrepancies between our two calculations reported here, one using the BDW amplitude and the other using the CGLN amplitude, are essentially due to the spin-independent part of the amplitude (which alone contributes to the coherent production) being different in the two cases. However, both the BDW and CGLN amplitudes yield comparable single nucleon cross sections for π^0 production, since in this case, an increase in the spin-independent term is compensated by a decrease in the spin-dependent part of the amplitude and vice versa.

There is again a reasonable agreement of the theory with the limited experimental data available⁶ for the angular distributions for ^4He as revealed by Figs. 6 and 7. As pointed out earlier, since the spin-independent terms of the CGLN and BDW amplitudes are almost the same near the resonance, the curve obtained with the CGLN amplitude almost overlaps with the one obtained with the BDW

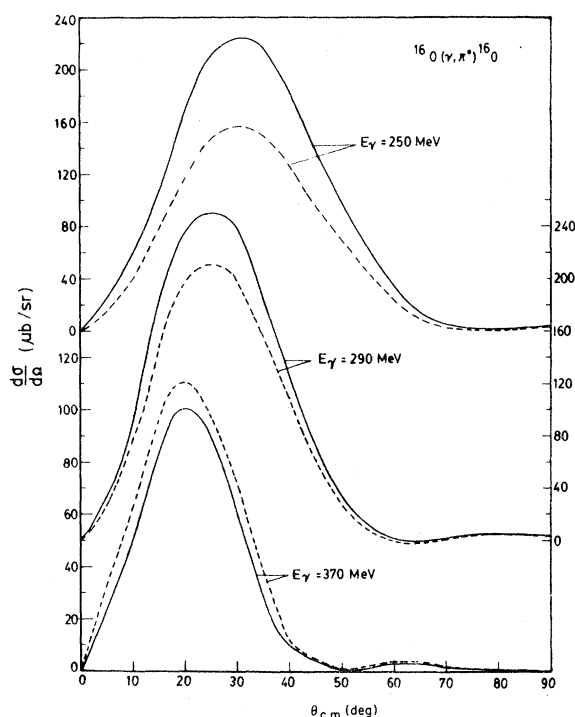


FIG. 4. Differential cross sections in DWIA for $^{16}\text{O}(\gamma, \pi^0)^{16}\text{O}$. The solid line indicates CGLN, the dashed line indicates BDW. The scale for the y axis is marked on the left for photon energies of 370 and 250 MeV, and on the right for the photon energy 290 MeV.

amplitude for $E_\gamma = 330$ MeV, and hence the former is not shown in Fig. 6. For the gamma energy of 290 MeV, the results with the CGLN amplitude vary only by about 10 to 20% and hence these are again not plotted in Fig. 6. The total cross sections shown for the nuclei ^{12}C , ^{16}O , and ^4He in Figs. 3, 5, and 8 establish the fact that the cross sections register a steep reduction with distortion in the resonance region, as expected. Our calculations for ^{40}Ca shown in Fig. 9, when compared to the results of Saunders, are in better agreement with the available data.² The noticeable disagreement of our theory with Davidson's data for ^{40}Ca and ^{12}C at the backward angles may be due to the poor resolution of the π^0 energy leading to an undetermined contribution from final nuclear states other than the ground states. The simple oscillator wave functions yield cross sections which are almost the same as those obtained with the Gaussian distribution for ^4He and Fermi distributions for ^{12}C , ^{16}O , and ^{40}Ca .

In conclusion, we wish to state that in the present theory, the pion production part does not involve any parametrization. The effect due to the change in pion momentum in the nuclear medium has also

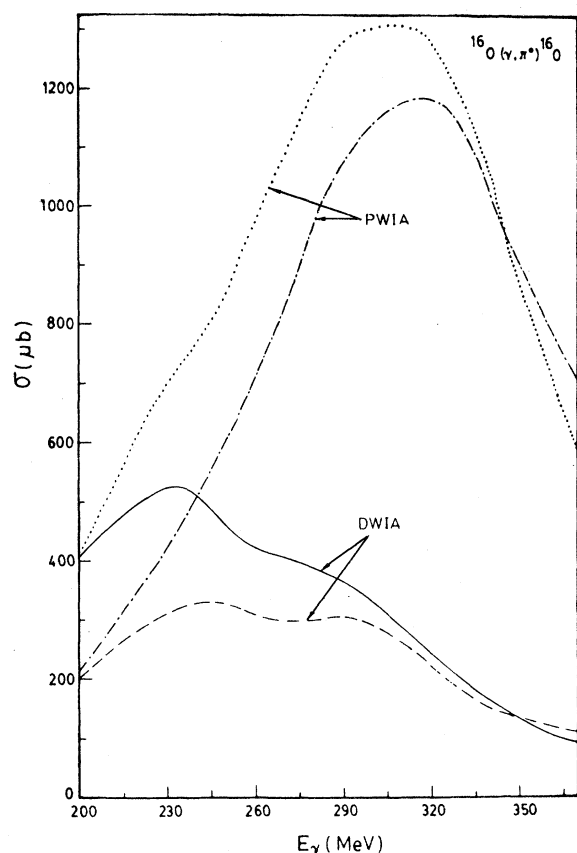


FIG. 5. Cross sections as a function of photon energy for $^{16}\text{O}(\gamma, \pi^0)^{16}\text{O}$. The dotted and continuous lines are arrived at by using the CGLN amplitude. The dashed-dotted and dashed lines are obtained with the BDW amplitude.

been taken into account. Proper care is taken of the final state interaction, the theory thereby predicting the cross sections much better than Saunders's DWIA calculation. The treatment by the latter of the final state interaction is rather crude. Although in the vicinity of the (3,3) resonance region, the π^0 production goes mainly through the Δ production, as has been substantiated by Saharia and Woloshyn, both the IDM and the present calculations are consistent and explain the data reasonably well for the simple reason that in both cases the parameters are determined by fitting the pion-nucleus elastic scattering data.

An interesting feature of the calculations is that there arises a large difference between the results obtained with the CGLN and BDW amplitudes. It appears that the CGLN amplitude provides a better explanation of the cross sections. It may be possible to reason why the CGLN works better by a rigorous testing of the two amplitudes against the polariza-

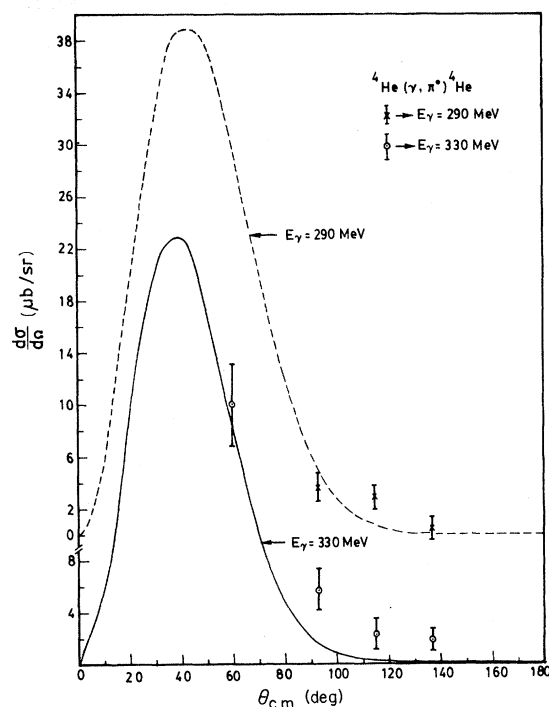


FIG. 6. Angular distribution for $^4\text{He}(\gamma, \pi^0)^4\text{He}$ compared with the data of Staples (as quoted by Saharia and Woloshyn). The BDW amplitude is used for the calculations.

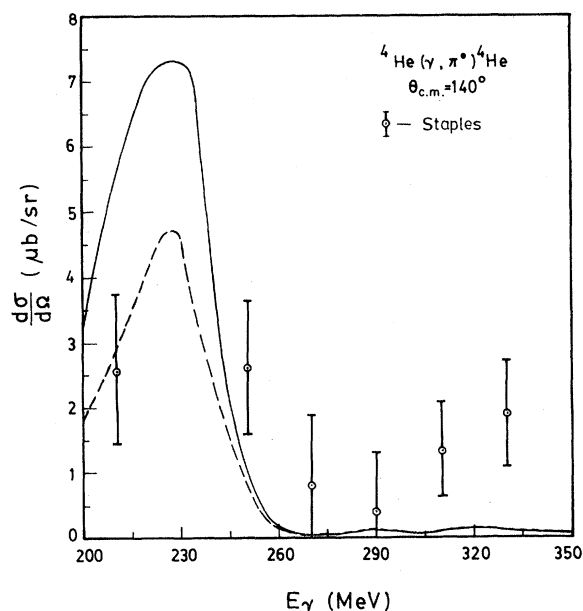


FIG. 7. Differential cross sections for pion angle $\theta_{c.m.} = 140^\circ$, along with the data of Staples as quoted by Saharia and Woloshyn (Ref. 4) for $\theta_{c.m.} = 137^\circ$. The full line and the dashed line are those obtained with the CGLN and BDW amplitudes, respectively.

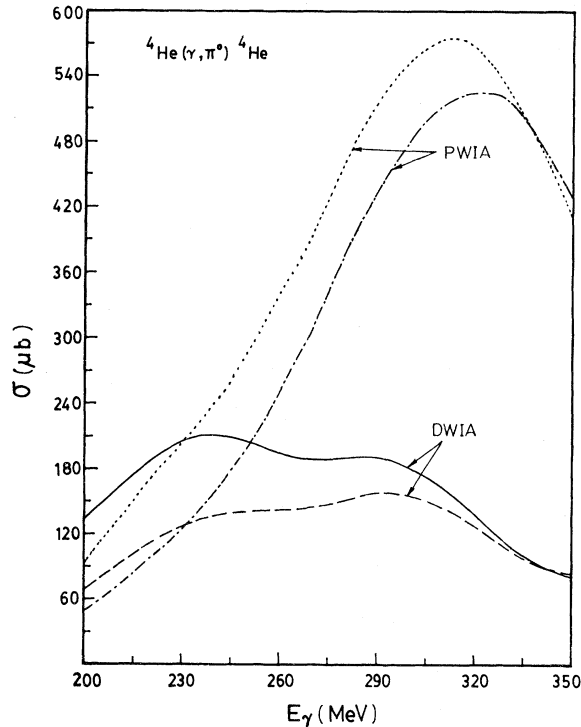


FIG. 8. Total cross sections for ${}^4\text{He}(\gamma, \pi^0){}^4\text{He}$. The other details are the same as Fig. 5.

tion data in addition to the data for the cross sections for production from single nucleons.

The present DWIA theory thus provides a reasonable agreement with the available sparse data. Systematic measurements of the differential and total cross sections would enable one to test the DWIA calculations and help one to distinguish the different elementary amplitudes.

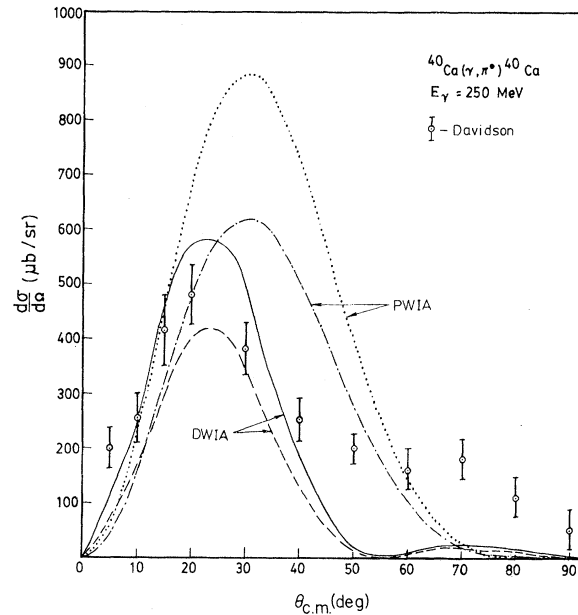


FIG. 9. Angular distribution for ${}^{40}\text{Ca}(\gamma, \pi^0){}^{40}\text{Ca}$, compared with the data of Davidson (as quoted by Saunders). See caption of Fig. 5 for other details.

ACKNOWLEDGMENTS

This work was in part supported by the Department of Atomic Energy, India. One of the authors (V.G.) wishes to thank Professor H. Überall and Dr. A. Nagl for their kind hospitality during her stay in Washington D.C., under the support of a National Science Foundation Grant to the Catholic University of America.

¹L. M. Saunders, Nucl. Phys. **B7**, 293 (1968).

²G. Davidson, Ph.D. thesis, Massachusetts Institute of Technology, 1959.

³R. M. Woloshyn, Phys. Rev. C **18**, 1056 (1978).

⁴A. N. Salaria and R. M. Woloshyn, Phys. Rev. C **23**, 351 (1981).

⁵L. S. Kisslinger and W. L. Wang, Ann. Phys. (N.Y.) **99**, 374 (1976).

⁶J. W. Staples, Ph.D. thesis, University of Illinois, 1969 (unpublished).

⁷R. A. Eisenstein and F. Tabakin, Comput. Phys. Commun. **12**, 237 (1976).

⁸J. Arends *et al.*, in *Abstracts of Contributed Papers to the IX International Conference on High Energy Physics and Nuclear Structure, Versailles, 1981*, edited by P. Catillon, P. Radvanyi, and M. Porneuf (North-

Holland, Amsterdam, 1982).

⁹B. L. Roberts *et al.*, in *Abstracts of Contributed Papers to the IX International Conference on High Energy Physics and Nuclear Structure, Versailles, 1981*, edited by P. Catillon, P. Radvanyi, and M. Porneuf (North-Holland, Amsterdam, 1982).

¹⁰F. A. Berends, A. Donnachie, and D. L. Weaver, Nucl. Phys. **B4**, 1 (1967); **B4**, 54 (1967); **B4**, 103 (1967).

¹¹G. F. Chew, M. L. Goldberger, F. E. Low, and Y. Nambu, Phys. Rev. **106**, 1345 (1967).

¹²M. E. Rose, *Elementary Theory of Angular Momentum* (Wiley, New York, 1957).

¹³K. Stricker, M. McManus, and J. A. Carr, Phys. Rev. C **19**, 929 (1979).

¹⁴V. Girijsa, Ph.D. thesis, University of Madras, 1982.